European Journal of Pharmaceutics and Biopharmaceutics 76 (2010) 1–9

Contents lists available at ScienceDirect

European Journal of Pharmaceutics and Biopharmaceutics

journal homepage: www.elsevier.com/locate/ejpb

Research paper

Matrix-loaded biodegradable gelatin nanoparticles as new approach to improve drug loading and delivery

Kenneth Ofokansi [a,b,c,*], Gerhard Winter [a], Gert Fricker [b], Conrad Coester [a,b]

[a] Department of Pharmacy, Pharmaceutical Technology and Biopharmaceutics, Ludwig-Maximilians University, Munich, Germany
[b] Department of Pharmaceutical Technology and Biopharmaceutics, Ruprecht-Karls University, Heidelberg, Germany
[c] Department of Pharmaceutics, University of Nigeria, Enugu State, Nigeria

ARTICLE INFO

Article history:
Received 28 August 2009
Accepted in revised form 19 April 2010
Available online 24 April 2010

Keywords:
Nanoparticles
Gelatin
FITC-dextran
Matrix loading
Loading capacity
Release characteristics
In vitro cell uptake

ABSTRACT

The long-term objective of this study is to develop a nanoparticulate formulation based on gelatin or its admixtures with other polyelectrolytes, under very gentle nanoprecipitation conditions, for the delivery of fragile macromolecules such as proteins and peptide drugs. However, the objective of the present study was to achieve drug loading into the matrices of gelatin-based nanoparticles through incubation of the drug-gelatin solution prior to formation and cross-linking of the nanoparticles in situ. Two molecular weight types (4 kDa and 20 kDa) of fluorescein isothiocyanate dextran (FITC-D) were used as surrogate macromolecules to study the loading and *in vitro* release behavior of gelatin nanoparticles. Unloaded and FITC-D-loaded gelatin nanoparticles were prepared by the one-step desolvation technique using ethanol–water mixture as the non-solvent. The preparation method was optimized with respect to the amount of cross-linking agent and cross-linking time. The nanoparticles formed were further characterized for mean size, size distribution and zeta potential using a Zetasizer nano while the morphology of the particles was evaluated by scanning electron microscopy (SEM). For cell uptake studies, FITC-D-labeled nanoparticles were incubated with Caco-2 cell monolayers and then evaluated using fluorescence microscopy. Results obtained showed the formation of very smooth and spherical particles with a unimodal distribution. Zeta potential measurements revealed that both the unloaded and FITC-D-loaded nanoparticles had a surface charge of −23.0 mV at pH 7.0. The loading capacity of the nanoparticles was found to be approximately 93.0 μg FITC-D (20 kDa) and 86 μg FITC-D (4 kDa) per milligram gelatin nanoparticles. Up to 16.5% of the 20 kDa FITC-D was loaded on the surface of the nanoparticles while 76.8% was entrapped into the matrices of the particles. For the 4 kDa FITC-D, 10.8% was bound to the surface of the particles while 75.6% was entrapped into the core of the nanoparticles. The release profile of FITC-D from the nanoparticles over a 168-h period showed a low release in phosphate-buffered saline (PBS), pH 7.4 while more than 80% was released after 3 h for both types of FITC-D in PBS containing trypsin. Release of the 4 kDa FITC-D from the nanoparticles was generally more rapid than that of the 20 kDa indicating that its entrapment into gelatin nanoparticles was based on weaker interactions when compared to that of the higher molecular weight FITC-D. Bio-imaging using fluorescence microscopy demonstrated uptake and internalization of the nanoparticles, notably into the nucleus and the cytoplasm, by Caco-2 cells.

1. Introduction

Colloidal drug carrier systems offer unending possibilities for drug targeting by a modified body distribution as well as the enhancement of cellular uptake of a number of substances [1,2]. As a result, undesirable side effects of the free drug can be potentially avoided especially for anti-cancer drugs such as methotrexate [3]. Biodegradable nanoparticles can be formulated from selected natural or synthetic macromolecules such as serum albumin, polycyanoacrylates, poly (lactic-co-glycolic) acid and recently chitosan. The use of gelatin as biomaterial for the formulation of colloidal drug delivery systems has severally been investigated by many authors [4–11].

Gelatin is a naturally occurring polymer with relatively low antigenicity [12] and has been used for decades in parenteral formulations and as an approved plasma expander. In addition, its biodegradability, biocompatibility, non-toxicity, ease of chemical modification and cross-linking make gelatin-based nanoparticles

* Corresponding author at: Department of Pharmaceutics, Faculty of Pharmaceutical Sciences, University of Nigeria, 410001 Nsukka, Enugu State, Nigeria. Tel.: +49 1744133869, +234 8037794874; fax: +49 89218077026, +234 42 770823.
E-mail addresses: kcofokansi@yahoo.com, kenneth.c.ofokansi@cup.uni-muenchen.de, ofokansi@uni-heidelberg.de (K. Ofokansi).

0939-6411/$ - see front matter © 2010 Elsevier B.V. All rights reserved.
doi:10.1016/j.ejpb.2010.04.008

a promising carrier system for drug delivery. In the field of immunotherapy, gelatin nanoparticles have been utilized to target CpG oligonucleotides to the lymph node in order to elicit a more efficient antitumoral immunity [13]. In a similar study, cationized gelatin nanoparticles have been found to strongly increase the immunostimulatory effects of CpG oligonucleotides [14]. Nanoparticles based on recombinant human gelatin have recently been prepared and its cytotoxicity compared with that prepared from type A gelatin [15]. Characteristic features of gelatin are a high content of the amino acids glycine, proline (mainly as hydroxyproline) and alanine which occur in repeating sequences and which confer on gelatin its triple helical structure. Commercial gelatin is a heterogeneous protein mixture of polypeptide chains and has a wide range of molecular weight ranging from a few thousand to several hundred thousand, even up to a few million Daltons [16–18]. The primary structure of gelatin offers many possibilities for chemical modification and covalent drug attachment. This can be done either within the matrix of the particles or on the surface of the particles only. In the former case, chemical modifications have to be done to the gelatin macromolecules before nanoparticles are formed, while in the latter case, the surface of the particles is used [19].

Although nanoparticulate colloidal systems based on gelatin have had much success as target-oriented protein-based drug delivery carriers in recent years, much of the drug loading achieved especially with DNA oligonucleotides and biotinylated peptide nucleic acid (PNA) had been on the surface of gelatin or modified gelatin nanoparticles and usually carried out after the preparation of the nanoparticles [17,20,21]. However, in order to be able to serve as an effective colloidal carrier for large dose drugs, loading of such drugs into the nanoparticles' matrices, in addition to surface loading, would significantly improve the loading capacity of the nanoparticles and subsequently lead to a better controlled release of the incorporated drug. Much of the research of our group has focused on exploring the versatility of gelatin as a polymeric colloidal carrier system. In our previous studies [22–25], gelatin nanoparticles had been successfully and reproducibly prepared by the two-step desolvation technique at either an acidic or an alkaline pH using acetone as the non-solvent. In view of the long-term goal of this study, the focus of the present work is to achieve drug loading into the matrices of the nanoparticles through incubation of the drug and gelatin solutions prior to formation and cross-linking of the nanoparticles at a neutral pH where virtually all drugs and especially peptides would be expected to retain, at least, their native structures and bioactivities, both during the preparation and on storage after preparation.

Characterization of drug loading with respect to surface-bound and matrix-entrapped drug for gelatin-based nanoparticulate formulations has not previously been reported. It is probable that a deeper understanding of the loading behavior of drugs into nanoparticles will be of immense benefit in elucidating the release mechanisms of such drugs from various polymeric systems. In the present study, we offer fresh insights into the loading behavior of macromolecules into polymeric nanoparticles using gelatin as our polymer of choice. For the first time, we have quantitatively differentiated between the amounts of surface-loaded and matrix-entrapped drug on gelatin nanoparticles using both low and medium molecular weight FITC-D (4 kDa and 20 kDa) as model macromolecules. The human colon adenocarcinoma cell line, Caco-2, has features similar to the absorptive intestinal cells, such as microvilli, the carrier-mediated transport systems, and paracellular transport through the tight junctions. Caco-2 cell monolayers have, therefore, been used as an *in vitro* model to study drug absorption [26], binding characteristics [27] and metabolism [28]. In an earlier study, FITC-D, 4.4 kDa, had been used as a model macromolecule to evaluate the efficacy of its cellular uptake in a colon cell layer model [29]. We have also, in this study, used Caco-2 cell monolayers as an *in vitro* model to investigate the uptake of the formulated nanoparticles.

2. Materials and methods

2.1. Materials

Gelatin type B from bovine skin (225 Bloom), glutaraldehyde grade 1 (25% aqueous solution), fluorescein isothiocyanate-labeled dextran (4 kDa and 20 kDa) and trypsin were obtained from Sigma–Aldrich Chemie, Steinheim, Germany. Ethyl alcohol was purchased from Fluka Chemie, Germany. All other reagents and chemicals were analytical grade and used as received.

2.2. Preparation of gelatin nanoparticles

Unloaded gelatin nanoparticles were prepared by the one-step desolvation method which was a modification of the two-step desolvation technique as previously reported [26]. Briefly, 200 mg of gelatin was dissolved in 20 ml of highly purified water (MilliQ™) at 37 °C under magnetic stirring (400 rpm) until a clear solution was obtained. The pH of the resulting solution was adjusted to between 6.1 and 8.0 with 0.2 M NaOH and incubated at 37 °C for 90 min. Hydroalcoholic solutions, similarly incubated, were then added to the gelatin solution over 3 min as the non-solvent to give final mixtures containing 0.2%w/w gelatin and between 65 and 70%w/w ethanol. The mixtures were incubated at 37 °C for a further 20 min and diluted 1:15 by weight, while stirring, with hydroalcoholic solutions of similar composition and at the same temperature but containing 200 μl of 25% aqueous solution of glutaraldehyde to cross-link the particles in situ. The above preparation method was further optimized with respect to the amount of cross-linking agent and cross-linking time and with respect to the optimal pH and ethanol concentration for preparation of the nanoparticles.

2.3. Preparation of FITC-dextran loaded gelatin nanoparticles

For the preparation of FITC-D loaded gelatin nanoparticles, 10 ml each of FITC-D (Mol. Wt.: 4 kDa and 20 kDa) solution was separately added to different flasks containing gelatin solution (20 mg/ml) and incubated at 37 °C under gentle magnetic stirring (200 rpm) for 90 min. The pH of the solution was then adjusted to 7.0 with 0.2 M NaOH and further incubated for 90 min before desolvation with ethanol–water mixture (70:30) as the non-solvent. The procedure was continued as described in section 2.2.

2.4. Characterization of the nanoparticles

The nanoparticle yield was determined gravimetrically by drying 400 μl nanoparticle dispersion in an oven at 60 °C until the weight became constant after about 3 h. The particle size of the nanoparticles was determined by photon correlation spectroscopy using a Zetasizer nano (ZEN 3600, Malvern, UK). For particle size analysis, the samples were measured in suspension after particle preparation and further necessary dilutions using highly purified water. Measurements were carried out at 25 °C at a light-scattering detection angle of 90°. The mean particle size and polydispersity index were determined. The zeta potential was similarly determined using a Zetasizer by phase analysis light scattering (PALS). Measurements of particle size, size distribution and zeta potential were similarly further monitored simultaneously at different pH using a Zetasizer to which an automatic pH multiple titrator (Malvern, UK) was coupled.

The surface morphology of the nanoparticles was determined by scanning electron microscopy (SEM) using a field emission scanning electron microscope (JSM-6500F, JEOL Instruments, Tokyo, Japan). The nanoparticles, in suspension, were mounted on metal grids, dried in a hot air oven at 60 °C, sputter-coated with carbon under vacuum and observed at an accelerating voltage of 4 kV and a working distance of 6 mm.

2.5. Evaluation of FITC-dextran loading into gelatin nanoparticles

To determine the amount of unentrapped and loaded FITC-D, the nanoparticles were separated by removing ethanol and residual low-molecular weight gelatin fractions by ultrafiltration through a 0.2-μm RC membrane (Sartorius, Germany) and using a 0.1% Tween 20 as the washing agent. The ultrafiltrate was immediately assayed for FITC-D by measuring the fluorescent intensity at excitation and emission wavelengths of 495 and 517 nm respectively using a fluorescence spectrophotometer (Cary-Eclipse, USA) to obtain the amount of unbound FITC-D. The recovered residue was redispersed in MilliQ water and shaken for 1 h at 300 rpm in a thermomixer (Eppendorf, Germany) to dissolve any FITC-D adsorbed on the surface of the particles. The resulting dispersion was centrifuged at 14,000*g* for 20 min and the fluorescent intensity of the supernatant measured to obtain the amount of FITC-D bound to the surface of the particles. The sediment was finally dispersed in 5 ml of trypsin solution (0.4 mg/ml) and shaken until a clear colourless solution was obtained which indicated a complete digestion of the gelatin nanoparticles and release of all FITC-D entrapped in the matrices (core) of the particles. The loading capacity of FITC-D was calculated from the obtained values.

2.6. In vitro release of FITC-dextran from the nanoparticles

The *in vitro* release of FITC-D was performed separately for 168 h in both phosphate-buffered saline (PBS) without enzyme, pH 7.4 and in PBS containing trypsin (5:1) at 37 ± 0.2 °C in a thermostated shaker agitated at 50 rpm. Approximately 40.2 mg of sedimented FITC-D-loaded gelatin nanoparticles were resuspended in 4.0 ml of PBS or PBS containing trypsin. At definite intervals of time, the particles were centrifuged at 14,000*g* for 5 min and 200 μl of the resulting supernatant was removed. The PBS and PBS containing trypsin solutions were replaced each time after each withdrawal in the respective falcon tubes to maintain a constant volume. The fluorescent intensity of the supernatant withdrawn at different time intervals was measured after appropriate dilutions. The amounts of the released FITC-D were then determined from a calibration plot previously established for the drug.

2.7. In vitro cell uptake studies

Caco-2 cells were cultured in 75-mL flasks (Corning, Acton, MA, USA) at 37 °C in an atmosphere of 5% CO2, 95% air and 95% relative humidity using Dulbecco's modified Eagle's medium (DMEM FG 0345, pH 7.4, Biochrom AG, Germany) supplemented with 10% fetal bovine serum, 1% non-essential amino acids, 1% L-glutamine, 1 mM sodium pyruvate, benzylpenicillin (100 U/mL), streptomycin sulphate (0.1 mg/mL) and 0.1% ciprofloxacin as the culture medium. The culture medium was replaced every 48 h. The cells (passage 29) were seeded on μ-slide 8 wells (Integrated Biodiagnostics, Germany, growth area 1.1 cm^2) at a seeding density of 9×104 cells/cm^2 and allowed to grow to confluency 48 h after seeding. The cells in each well were then incubated with 300 μL of 10 mg/mL suspension of FITC-D (20 kDa)-loaded nanoparticles for one 90 min. After removal of the nanoparticle suspension by aspiration, the cells were rinsed thrice with PBS, pH 7.4, and then fixed by adding 300 μL of 4% p-formaldehyde for 30 min and thereafter rinsed thrice with PBS. A control experiment was also set up in which the cells were treated with equivalent concentration (0.0113%) of FITC-D solution for the same duration under the same conditions before being fixed with formaldehyde. The cell samples were then viewed in a fluorescence microscope (Modell BZ 8000, Keyence, Germany) to capture both the bright field and fluorescence images of the cells. In order to obtain a clearer picture on the location of the uptaken nanoparticles within the cells, a fluorescent nuclear stain 4′-6-Diamidino-2-phenylindole (DAPI) was used to stain the cells. For nuclear staining with DAPI, the cells after being fixed with p-formaldehyde and washed thrice with PBS were permeabilized by incubation with 0.1% Triton-X 100 in PBS for 10 min followed by washing thrice with PBS. Finally, DAPI in PBS (1:9) was added to each of the wells and incubated at room temperature for 10 min and then washed thrice with PBS before viewing in a fluorescence microscope.

3. Results and discussion

3.1. Preparation and characterization of the nanoparticles

Preliminary experiments carried out using 1 ml of glyoxal to cross-link the gelatin nanoparticles as reported by earlier investigators [7] resulted in instantaneous mass aggregation and precipitation of the nanoparticles. Hence, glutaraldehyde was employed to cross-link the nanoparticles in situ. Glutaraldehyde is a non-zero length cross-linker which induces poly- or bi-functional cross-links into the network structure of some biopolymers by bridging free amino groups of lysine or hydroxyl lysine of protein-based biopolymers such as gelatin. No aggregation or precipitation of particles occurred on addition of glutaraldehyde and the resulting particles remained stable after the processing and washing steps for more than 10 months on storage under refrigeration conditions at 2–8 °C. The one-step desolvation technique is a new simplified preparation approach in which it is no longer necessary to perform an initial desolvation step to discard the low-molecular weight gelatin fraction. Thus, gelatin was dissolved at a certain concentration under constant mild heating and stirring (37 °C; 500 rpm). Contrary to the gelatin solution before the usual second desolvation step, the pH was now adjusted to neutral values before nanoparticles were generated by addition of ethanol. Gelatin, therefore, does not necessarily have to contain an increased amount of high-molecular weight components for the production of stable and homogeneous colloidal spheres as stated by earlier authors [30]. The temperature of preparation of the nanoparticles (37 °C) was selected to ensure that the molecular weight distribution of gelatin remained relatively constant during incubation [30]. Similarly, the selected pH of 7.0 which was clearly above the isoelectric point of type B gelatin (IEP of 4.7–5.2) had to be such that the gelatin molecules would be sufficiently uncharged to remain sensitive to desolvation but sufficiently charged to prevent their aggregation during nanoparticle formation. The mean particle size of the unloaded and FITC-D-loaded gelatin nanoparticles as determined by photon correlation spectroscopy was found to be 253 and 281 nm (mean of 28 sub-runs) respectively with a narrow-size distribution. The optimum amount of glutaraldehyde needed for effective cross-linking of the nanoparticles was found to be 37.5 mg per 200 mg of gelatin. This amount of glutaraldehyde yielded particles with the lowest mean size of 253 nm and polydispersity index (PI) of 0.073 (Table 1). Amounts of glutaraldehyde lower or higher than this optimum yielded nanoparticles of higher mean size and PI. It is worthy of note that in this proposed new production method, 37.5 mg glutaraldehyde per 200 mg gelatin was found to be the optimal amount for cross-linking the nanoparticles whereas in the two-step desolvation technique, lower

Table 1
Variation of mean size and polydispersity index of the gelatin nanoparticles with amount of cross-linking agent.

	Amount of cross-linking agent (mg)							
	25.0	31.25	37.5	43.75	50.0	56.25	62.5	68.75
Mean size* (nm)	322 ± 8.0	341 ± 13.0	273 ± 13.0	336 ± 9.0	479 ± 25.0	334 ± 4.0	313 ± 22.0	392 ± 32.0
Polydispersity index	0.110 ± 0.04	0.098 ± 0.003	0.073 ± 0.011	0.251 ± 0.032	0.229 ± 0.013	0.133 ± 0.088	0.225 ± 0.106	0.100 ± 0.068

* Mean size and polydispersity index are mean ± SD of 28 sub-runs.

Table 2
Mean size and polydispersity index of the gelatin nanoparticles as a function of cross-linking time.

	Time (min)							
	5	10	20	30	40	50	60	70
Mean size[a] (nm)	2250 ± 1060	296[b] ± 6.0	297[b] ± 5.0	289[b] ± 9.0	295[b] ± 2.0	273[b] ± 1.0	284[b] ± 14.0	292[b] ± 5.0
Polydispersity index	0.123 ± 0.013	0.125 ± 0.003	0.115 ± 0.018	0.152 ± 0.027	0.101 ± 0.019	0.073 ± 0.009	0.107 ± 0.008	0.094 ± 0.008

[a] Mean size and polydispersity index are mean ± SD of 28 sub-runs.
[b] At $p < 0.05$, there was no significant difference in the mean sizes of the particles within a cross-linking time of 10–70 min.

amount (43.75 mg) of glutaraldehyde was found to be optimal. The variation of mean size and PI as a function of the cross-linking time is shown in Table 2. A cross-linking time of 5 min was found to be inadequate for type B gelatin nanoparticles as is evident in the very high mean size of the resulting particles. This batch also showed early signs of instability manifested as cloudy precipitate when left to stand for a few minutes after cross-linking. Within a cross-linking time range of 10–70 min, stable nanoparticles with no significant difference ($P < 0.05$) in the particle mean size were formed. A cross-linking time of 50 min, however, yielded nanoparticles with the most narrow-size distribution. Therefore, a cross-linking time of 50 min was used in subsequent experiments before any unreacted glutaraldehyde was quenched by the addition of a solution of 12% sodium metabisulphite.

We further investigated the effect of formulation pH on the particle size, polydispersity index and zeta potential where the polydispersity index measures the second moment of the size distribution of the nanoparticle population. The effect of the formulation pH on these parameters is illustrated in Figs. 1 and 2. A lower PI indicates a narrow-size distribution. Previous reports

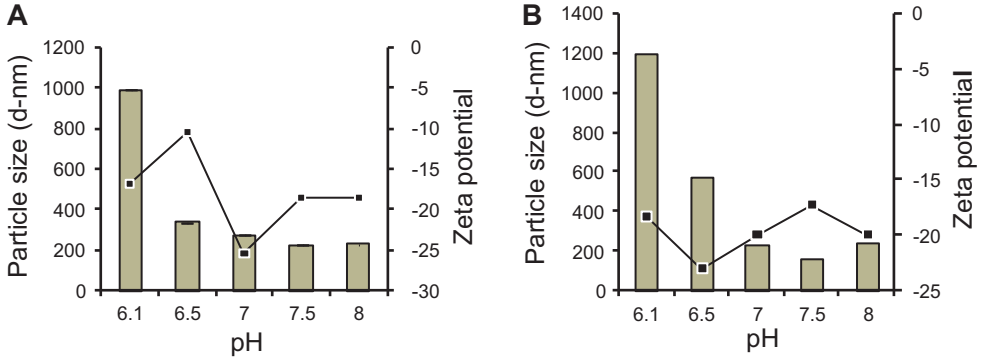

Fig. 1. Variation of formulation pH with particle size and zeta potential for gelatin nanoparticles prepared with 70%w/w ethanol (A) and 65%w/w ethanol (B) as non-solvent.

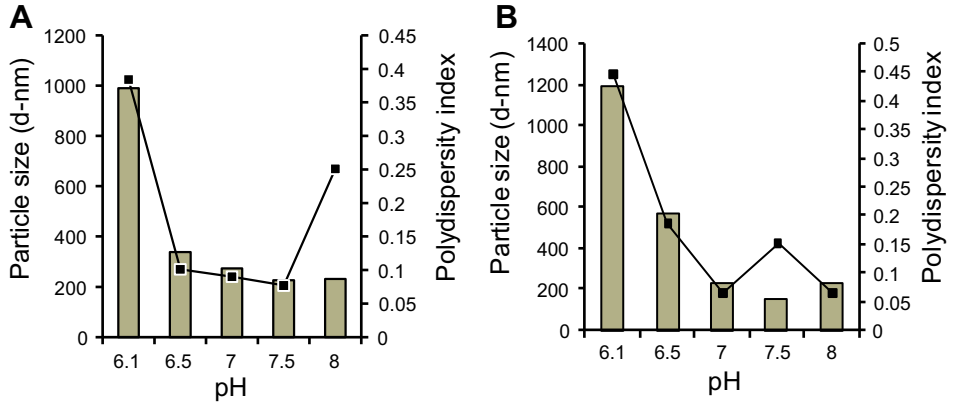

Fig. 2. Variation of formulation pH with particle size and polydispersity index for gelatin nanoparticles prepared with 70%w/w ethanol (A) and 65%w/w ethanol (B) as non-solvent. (For interpretation of the references to color in this figure legend, the reader is referred to the web version of this article.)

[27] had established that ethanol concentrations between 65%w/w and 70%w/w yielded gelatin nanoparticles of predictably smaller particle size and narrow-size distribution (lower PI). Concentrations of ethanol lower or higher than this optimum range led to insufficient scattering when measured by photon correlation spectroscopy due to low nanoparticle yield or to formation of particles having a wide-size distribution (high PI). At formulation pH of 6.1 for both 65%v/v and 70%v/v ethanol, particles having a high mean size which tended to go beyond the nanometer size range were formed. Although particles less than 200 nm in size and of narrow-size distribution were formed at the pH of 7.5 and 8.0, the nanoparticle yield as evaluated from gravimetric measurements was low (data not shown). At the pH of 6.5 and 7.0, nanoparticles with desired characteristics with respect to particle size, size distribution and nanoparticle yield were formed (Figs. 1 and 2). However, we subsequently chose to further evaluate the formulations prepared at pH 7.0 in view of its better long-term attraction especially for the encapsulation and delivery of peptides where a neutral pH would be expected to offer potential advantages in terms of its inherent capacity for the preservation of the chemical stability of such fragile macromolecules.

The SEM photomicrographs of the unloaded and FITC-D-loaded nanoparticles as shown in Fig. 3 confirm the formation of spherical nanoparticles with very smooth surfaces. Zeta potential measurements revealed that the unloaded gelatin nanoparticles had a surface charge of −23.0 mV at pH 7.0 (Figs. 1 and 2). Loading of FITC-D into the nanoparticles had no effect on the surface charge of the particles. This was anticipated since FITC-D, being a neutral molecule, would not be expected to alter the surface charge of the nanoparticles. The effect of pH on the zeta potential and mean size of the particles was further monitored using a Zetasizer to which a pH multiple titrator was coupled to form an easy-to-use assembly which could automatically and simultaneously monitor the zeta potential and the mean size of nanoparticle dispersion at any selected range of pH. The result of this investigation is shown in Fig. 4. At acidic pH range (1–4.5) which corresponded to pH values below the IEP of type B gelatin, the nanoparticles exhibited a positive surface charge whereas negative zeta potential values were recorded above the pH of 5 corresponding also to pH values above the IEP of type B gelatin showing the dependency of the surface charge of gelatin nanoparticles on pH. The mean particle size increased marginally with increasing pH over the pH range 3–12; an indication that the particle size of the nanoparticles after preparation is altered to some extent by changes in pH of the environment.

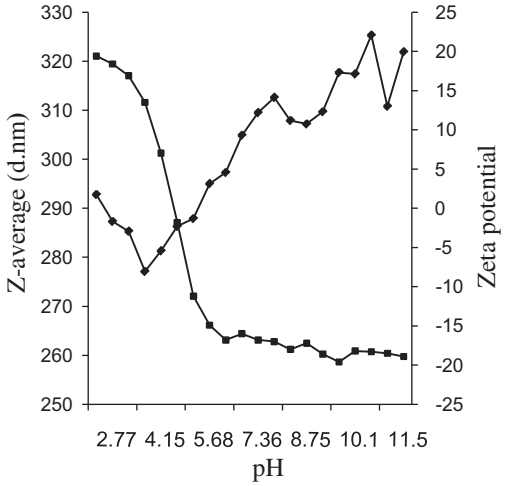

Fig. 4. Variation of pH with particle size and zeta potential for already prepared gelatin nanoparticles monitored simultaneously with a Zetasizer–pH multiple titrator assembly.

3.2. Loading of FITC-dextran into gelatin nanoparticles

The loading efficiency of the fluorescent dye-labeled dextran was determined by fluorescence spectrophotometry. For the amount of FITC-D entrapped into the matrix of the nanoparticles to be quantified, the pelletized particles after the last centrifugation step had to be broken down via enzymatic digestion using trypsin. Trypsin had previously been demonstrated to be the most effective enzyme for the disintegration of gelatin nanoparticles [4]. The loading capacity of the nanoparticles was calculated to be 86 and 93 μg per milligram gelatin for 4 kDa and 20 kDa FITC-D respectively which suggests a high loading capacity that would be suitable for improved drug dose delivery especially for macromolecules. These amounts corresponded to 86.4% and 93.3% of the total amounts of 4 kDa and 20 kDa FITC-D used in the loading study. A clearer picture of the loading behavior of the two molecular weight types of FITC-D is shown in Fig. 5. Up to 76.8% of the total amount of 20 kDa FITC-D was entrapped into the matrices (core) of the particles while 16.5% was loaded on the surface of the nanoparticles. The matrix-entrapped and surface-loaded amounts for 4 kDa FITC-D were respectively 75.7% and 10.8%. It can easily be discerned from Fig. 5 that only 4.3% of the total amount of 20 kDa FITC-D used for the encapsulation study was nei-

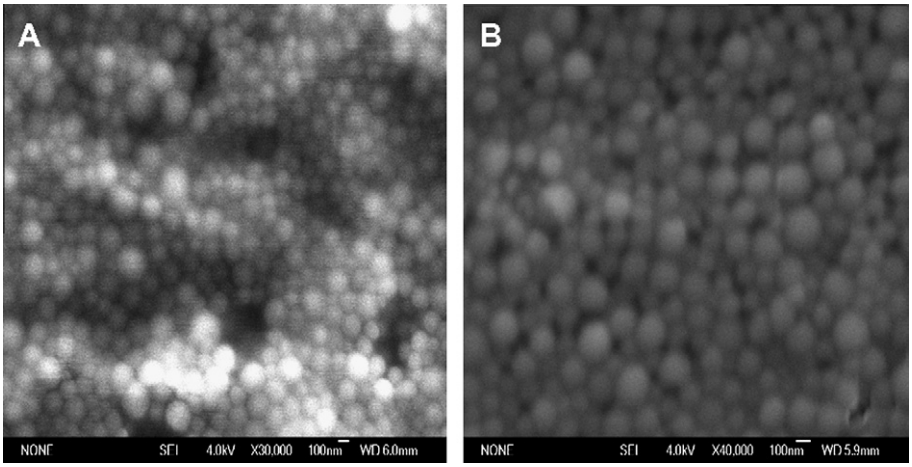

Fig. 3. SEM photomicrographs of FITC-D-loaded (A) and FITC-D-unloaded (B) gelatin nanoparticles showing very smooth and spherical particles.

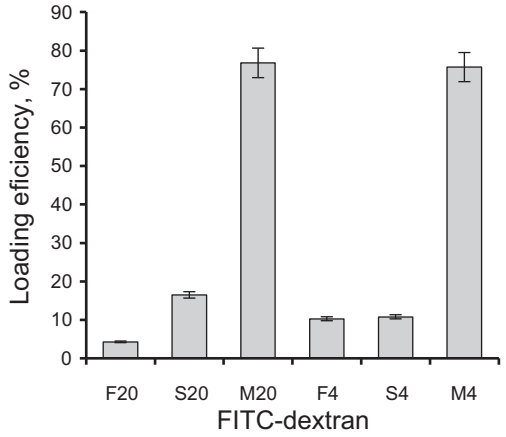

Fig. 5. Loading characteristics of FITC-D into gelatin nanoparticles. F20, S20, M20, F4, S4, M4 represent respectively free/unentrapped 20 kDa FITC-D, surface-loaded 20 kDa FITC-D, matrix-entrapped 20 kDa FITC-D, free/unentrapped 4 kDa FITC-D, surface-loaded 4 kDa FITC-D and matrix-entrapped 4 kDa FITC-D.

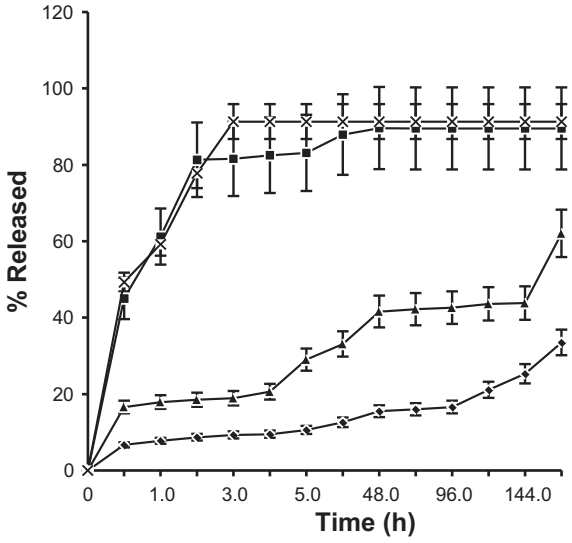

Fig. 6. Release profile of FITC-D from gelatin nanoparticles in PBS with and without enzyme. —♦— 20 kDa in PBS, —▲— 4 kDa in PBS, —■— 20 kDa in PBS containing trypsin, —×— 4 kDa in PBS containing trypsin.

ther entrapped in the matrix nor bound to the surface of the nanoparticles. For the 4 kDa FITC-D, approximately 10.3% of the total amount remained unentrapped by the nanoparticles. There appears, therefore, to be a higher entrapment for the larger molecular weight FITC-D (20 kDa) than the lower type (4 kDa). At $P = 0.05$, the differences in the respective entrapped amounts for both types of FITC-D were found to be significant. Furthermore, it is probable that the entrapment of FITC-D which is a neutral molecule to gelatin nanoparticles is due to non-covalent interactions since gelatin (type B, IEP = 4.7–5.2) remains largely negatively charged at a pH of 7.0. Non-covalent interactions unlike covalent types proceed more slowly and go to completion over time. To verify the effect of incubation of the solutions of FITC-D and gelatin prior to desolvation, nanoparticles were prepared following the mixing of the two solutions without any incubation. The loading behavior (data not shown) revealed significantly reduced amounts of both the surface-loaded and matrix-entrapped drugs for both types of FITC-D. The higher entrapment of 20 kDa FITC-D, in comparison with that of 4 kDa FITC-D, may also be an indication that its entrapment into gelatin nanoparticles is based on a higher number of interactions with the particles resulting probably from its larger molecular size.

3.3. In vitro release of FITC-dextran from the nanoparticles

The release of FITC-D from the gelatin nanoparticles was performed in PBS without enzyme, pH 7.4, and in PBS containing trypsin, pH 6.3, at 37 °C. The release profile in the two release media over a 168-h period is shown in Fig. 6. With PBS as release medium, there was a low release of both types of FITC-D even after 144 h. Over the whole release period, only 36% of the 20 kDa FITC-D was released while about 60% of the lower molecular weight type was released. Although the intensities of the interaction between the particles and both types of FITC-D may appear to be the same, it is probable that the slower release of FITC-D, 20 kDa, just like its higher loading efficiency, may also be due to a higher number of interactions with the particles resulting from its larger molecular size.

The t_{20}, which defines the time taken for 20% of the drug to be released, was calculated from Fig. 6 to be 4 and 120 h for 20 kDa and 4 kDa FITC-D, respectively. A burst release which occurred within the first 30 min of the release period accounted for 18% and 9% respectively of the total amount of 4 and 20 kDa FITC-D used in the release experiment in PBS. The respective amounts released as a result of the burst effect may likely represent the amounts bound to the surface of the gelatin nanoparticles. The remaining amounts which were released in a more gradual fashion over a longer period of time likely represented part of the FITC-D entrapped into the matrices of the nanoparticles. It is, therefore, not difficult to decipher a correlation between these results and that from the loading studies where 16.5% and 10.8% of the 20 and 4 kDa FITC-D respectively were found to be bound to the surface of the particles. Conversely, the release of FITC-D from the nanoparticles in PBS containing trypsin showed a pattern which contrasted sharply with the release behavior in PBS alone (Fig. 6). There was a burst release of about 48% of both types of FITC-D within the first 30 min, followed by a somewhat rapid release over the next 150 min. On the whole, more than 80% of both types of FITC-D was released after 3 h in the presence of trypsin. As earlier noted, trypsin is known to be the most effective enzyme for the digestion of gelatin nanoparticles. In the light of the observed release behavior of FITC-D from the nanoparticles, we can infer that the three predominant mechanisms of release of these macromolecules from gelatin nanoparticles are desorption, diffusion and nanoparticle erosion and/or disintegration. The initial burst release which was observed is believed to occur through a combination of one or more of desorption, diffusion, nanoparticle erosion and nanoparticle disintegration depending on the release medium employed. Overall, it is equally discernible from Fig. 6 that the release of 4 kDa FITC-D from the nanoparticles was generally more rapid than that of 20 kDa FITC-D; an indication that its entrapment into gelatin nanoparticles may be based on weaker interactions when compared to that of the higher molecular weight FITC-D.

3.4. In vitro cell uptake studies

A thorough understanding of intestinal epithelial transport is crucial for evaluating the potential for oral dosing of drug candidates. The Caco-2 permeability assay is considered the industry gold standard for *in vitro* prediction of *in vivo* human intestinal permeability and bioavailability of orally administered drugs [31,32]. Cellular uptake of the fluorescent-labeled nanoparticles was demonstrated by fluorescence microscopy using Caco-2 cell monolayers. We chose this cell line because of availability in addition to the fact that it is the gold standard for *in vitro* prediction of *in vivo* intestinal permeability and bioavailability of orally admin-

istered drugs. Moreover, our ultimate goal is to evaluate our nanoparticulate formulation as an oral delivery system for some peptides and protein drugs. Fig. 7 shows the cellular uptake and distribution of FITC-D-labeled gelatin nanoparticles with an average particle size of 280 nm by Caco-2 cells. In Fig. 7, A shows the detection of FITC-D-labeled nanoparticles, B shows the bright field image of the internalized particles in Caco-2 cells while C is an overlay of A and B. As shown in Fig. 7B, a good number of the labeled particles could be observed around the cytoplasm of the Caco-2 cells. As a control, when FITC-D solution was incubated with the cells under the same conditions, no free FITC-D was detected inside of the cells as shown in Fig. 7D. Taken together, our results show that FITC-D-labeled gelatin nanoparticles were taken up by Caco-2 cells whereas free FITC-D (not attached to the nanoparticles) was not detected. Nuclear staining of the cells, however, clearly showed that there was substantial internalization of the nanoparticles into the nucleus of the cells as shown in Fig. 7F and G. Fig. 7E shows the fluorescence image of the nuclei of Caco-2 cells as stained by DAPI. DAPI is a fluorescent nuclear stain excited by UV light and showing strong blue fluorescence when bound to DNA. It is known to form fluorescent complexes with natural double-stranded DNA, showing a fluorescence specificity for AT, AU and IC cluster. It has been demonstrated that the uptake of particulate systems can occur via various processes including phagocytosis, fluid phase pinocytosis or receptor-mediated endocytosis [9,10,33]. Recently, the transcytosis of nanoparticles has been reported by a number of authors. Behrens and co-workers showed that chitosan or polystyrene nanoparticles were taken up by enterocyte-like Caco-2 cells presumably in a transcytic manner [34]. They observed that the uptake of nanoparticles was significantly reduced under conditions that blocked active transport processes, for example 4 °C in the presence of sodium azide. Other investigators also identified the proteins involved in internalizing foreign materials inside polarized Caco-2 cells and proposed a possible transcytic transport mechanism across Caco-2 cells by the endosome-associated pathways [35]. In view of the results of these recent reports and the knowledge that the Caco-2 cell is a specialized cell that transports external molecules from an apical to the basolateral side, it is reasonable to postulate that the uptake of FITC-D-labeled nanoparticles in our present study was by a transcytic mechanism. This postulation is further supported by the fact that particle transport by the M cells is predominantly transcellu-

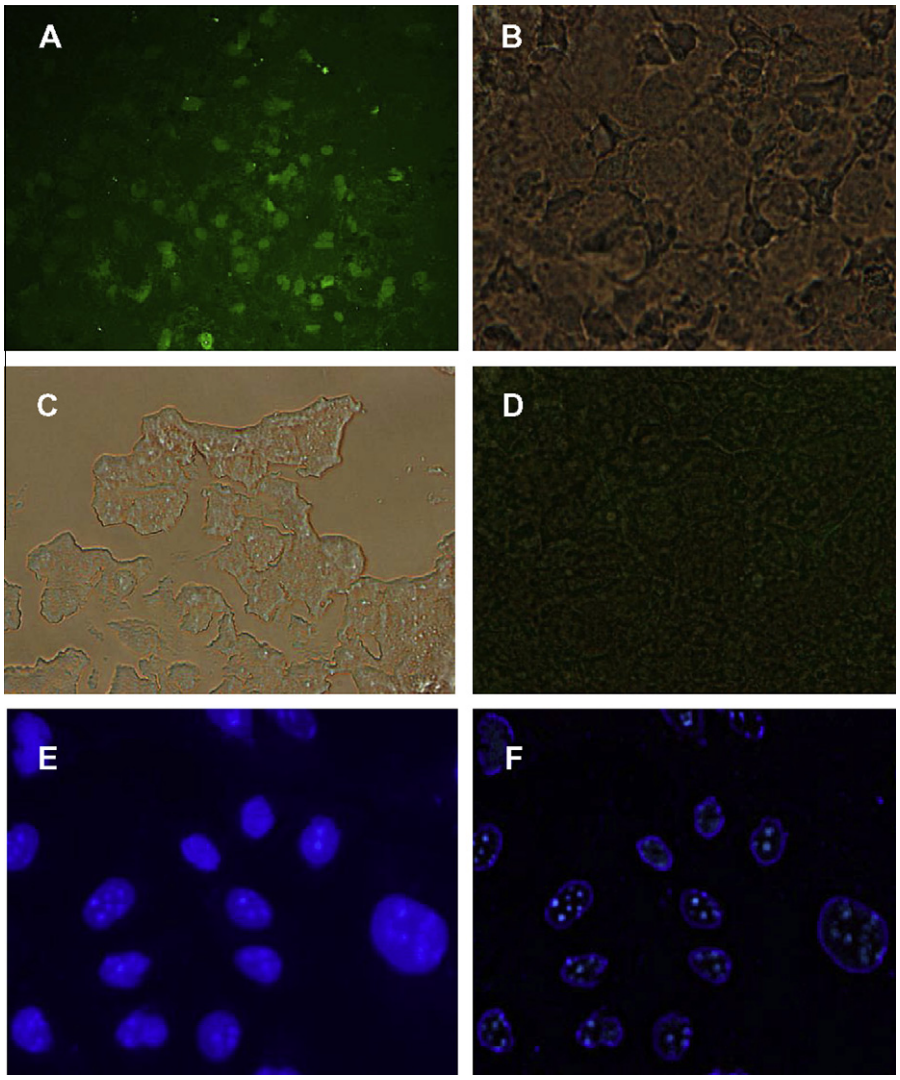

Fig. 7. Fluorescence images of Caco-2 cell monolayers after incubation with the FITC-D labelled nanoparticles for 60 mins. (A) Detection of FITC-D labelled nanoparticles, (B) Bright field image of up-taken FITC-D labelled nanoparticles in Caco-2 cells, (C) Overlap of A and B, (D) Control which is a bright field image of FITC-D incubated with the cells under the same conditions, (E) Nuclei of Caco-2 cells showing the internalization of nanoparticles after staining with DAPI, (F) Haze reduction image of (E) showing the internalized particles more clearly.

lar and energy dependent [36]. The transcellular transport of nanoparticles generally starts with the uptake by one of these endocytic mechanisms: pinocytosis, macropinocytosis, or clathrin-mediated endocytosis [37]. All of these are active processes, i.e., energy is required for the particle internalization. Both clathrin-mediated endocytosis and phagocytosis are receptor-mediated processes. Clathrin-mediated vesicles may internalize particles smaller than 150 nm [38]; while during phagocytosis particulate matters up to several μm may be internalized. Macropinocytosis is also an active, actin-dependent process, which is in many ways similar to phagocytosis, but is not receptor-mediated [39]. Larger volumes of fluid-containing particles can be internalized by macropinocytosis in vesicles of varying sizes but smaller than 5 μm. For a number of years, it has been widely accepted that nanoparticles with a hydrophobic surface should be taken up more extensively by the intestinal epithelium than those with hydrophilic surface [40]. However, recent studies have shown that other factors such as colloidal stability and mucoadhesion are capable of influencing nanoparticle uptake by intestinal cells. Some recent results have suggested that the presence of hydrophilic polymers on the surface of nanoparticles could increase the transport of these systems through mucosal surfaces [41]. The hydrophilicity of gelatin may have contributed to the observed uptake of our nanoparticles in the present study.

4. Conclusions

Improved loading of the neutral macromolecule, FITC-D, into the matrices of type B gelatin nanoparticles could be attained by incubation of the drug and gelatin solutions at 37 °C and pH 7.0 prior to desolvation in order to give adequate room for the non-covalent interaction between the two molecules to go to completion. Under these conditions, it can be concluded that effective and improved loading of high-molecular weight macromolecules into the matrices of gelatin nanoparticles is attainable as was evident in the loading and *in vitro* drug release studies. The loading and *in vitro* release characteristics were seen to be dependent on the molecular size of the FITC-D being loaded. Since Caco-2 cells have been widely used as an *in vitro* model to evaluate the paracellular permeability of macromolecules, the preliminary results obtained in the cell uptake studies using Caco-2 cells could be of significant importance in optimizing the gelatin-based nanoparticulate systems for the oral delivery of therapeutic agents including proteins, peptides and nucleic acids.

Acknowledgement

The authors are deeply grateful to the Alexander von Humboldt (AvH) Foundation for granting a post-doctoral Research Fellowship through which this research work was carried out.

References

[1] J. Kreuter, Evaluation of nanoparticles as drug-delivery systems II: comparison of the body distribution of nanoparticles with the body distribution of microspheres (diameter 1 μm), liposomes, and emulsions, Pharm. Acta Helv. 58 (1983) 217–226.
[2] V. Schäfer, H. von Briesen, R. Andressen, A.M. Steffan, C. Royer, S. Tröster, J. Kreuter, H. Rübsamen-Waigmann, Phagocytosis of nanoparticles by human immunodeficiency virus (HIV)-infected macrophages: a possibility for antiviral drug targeting, Pharm. Res. 9 (1992) 541–546.
[3] R. Narayani, K.P. Rao, Preparation, characterization and in vitro stability of hydrophilic gelatin microspheres using a gelatin–methotrexate conjugate, Int. J. Pharm. 95 (1993) 85–91.
[4] E. Leo, M.A. Vandelli, R. Cameroni, F. Forni, Doxorubicin-loaded gelatin nanoparticles stabilized by glutaraldehyde: involvement of the drug in the cross-linking process, Int. J. Pharm. 12 (1997) 75–82.
[5] T.K. Yeh, Z. Lu, M.G. Wientjes, J.L.S. Au, Formulating paclitaxel in nanoparticles alters its disposition, Pharm. Res. 22 (2005) 867–874.
[6] V.L. Truong-Le, S.M. Walch, E. Schweibert, H.Q. Mao, W.B. Guggino, J.T. August, K.W. Leong, Gene transfer by DNA–gelatin nanospheres, Arch. Biochem. Biophys. 361 (1999) 47–56.
[7] G. Kaul, M. Amiji, Cellular interactions and in vitro DNA transfection studies with poly(ethyleneglycol)-modified gelatin nanoparticles, J. Pharm. Sci. 94 (2005) 184–198.
[8] G. Kaul, M. Amiji, Tumour-targeted gene delivery using poly(ethyleneglycol)-modified gelatin nanoparticles: in vitro and in vivo studies, Pharm. Res. 22 (2005) 951–961.
[9] S. Balthasar, K. Michaelis, N. Dinauer, H. von Briesen, J. Kreuter, K. Langer, Preparation and characterization of antibody modified gelatin nanoparticles as drug carrier system for uptake in lymphocytes, Biomaterials 26 (2005) 2723–2732.
[10] N. Dinauer, S. Balthasar, C. Weber, J. Kreuter, K. Langer, H. von Briesen, Selective targeting of antibody-conjugated nanoparticles to leukemic cells and primary T-lymphocytes, Biomaterials 26 (2005) 5898–5906.
[11] K.C. Ofokansi, M.U. Adikwu, V.C. Okore, Preparation and evaluation of mucin–gelatin mucoadhesive microspheres for rectal delivery of ceftriaxone sodium, Drug Dev. Ind. Pharm. 33 (2007) 691–700.
[12] Y. Gabr, N. Assem, A. Michael, L. Fahmy, Evaluation studies on oxypolygelatin and degraded gelatin as plasma volume expander, Arzneimittelforschung 46 (1996) 763–766.
[13] C. Bourquin, D. Anz, K. Zwiorek, A.L. Lanz, S. Fuchs, S. Weigel, C. Wurzenberger, P. von der Borch, M. Golic, S. Moder, G. Winter, C. Coester, S. Endres, Targeting CpG oligonucleotides to the lymph node by nanoparticles elicits efficient antitumoral immunity, Journal of Immunology 181 (2008) 2990–2998.
[14] K. Zwiorek, C. Bourquin, J. Battiany, G. Winter, S. Endres, G. Hartmann, C. Coester, Delivery by cationic gelatin nanoparticles strongly increases the immunostimulatory effects of CpG oligonucleotides, Pharm. Res. 25 (2008) 551–562.
[15] Y.W. Won, Y.H. Kim, Preparation and cytotoxicity comparison of type A gelatin nanoparticles with recombinant human gelatin nanoparticles, Macromol. Res. 17 (2009) 464–468.
[16] A. Veis, The macromolecular chemistry of gelatin, Academic Press, New York, 1964.
[17] C.J. Coester, K. Langer, H. von Briesen, J. Kreuter, Gelatin nanoparticles by two step desolvation – a new preparation method, surface modifications and cell uptake, J. Microencapsul. 17 (2000) 187–193.
[18] W. Fraunhofer, G. Winter, C. Coester, Asymmetrical flow field-flow fractionation and multi-angle light scattering for analysis of gelatin nanoparticle drug carrier systems, Anal. Chem. 76 (2004) 1909–1920.
[19] C. Weber, C. Coester, J. Kreuter, K. Langer, Desolvation process and surface characterization of protein nanoparticles, Int. J. Pharm. 194 (2000) 91–102.
[20] K. Zwiorek, J. Kloeckner, E. Wagner, C. Coester, Gelatin nanoparticles as a new and simple gene delivery system, J. Pharm. Pharmaceut. Sci. 7 (2004) 22–28.
[21] J. Zillies, C. Coester, Evaluating gelatin based nanoparticles as a carrier for double stranded oligonucleotides, J. Pharm. Pharmaceut. Sci. 7 (2004) 17–21.
[22] C. Coester, P. Nayyar, J. Samuel, In vitro uptake of gelatin nanoparticles by murine dendritic cells and their intracellular localization, Eur. J. Pharm. Biopharm. 62 (2006) 306–314.
[23] C. Coester, J. Kreuter, H. von Briesen, K. Langer, Preparation of avidin-labelled gelatin nanoparticles as carriers for biotinylated peptide nucleic acid (PNA), Int. J. Pharm. 196 (2000) 147–149.
[24] J. Zillies, K. Zwiorek, G. Winter, C. Coester, Method for quantifying the PEGylation of gelatin nanoparticle drug carrier systems using asymmetrical flow field-flow fractionation and refractive index detection, Anal. Chem. 79 (2007) 4574–4580.
[25] K. Zwiorek, C. Bourquin, J. Battiany, G. Winter, G. Hartmann, C. Coester, Delivery by cationic gelatin nanoparticles strongly increases the immunostimulatory effects of CpG oligonucleotides, Pharm. Res. 25 (2008) 551–562.
[26] I.J. Hildago, J.B. Li, Carrier-mediated transport and efflux mechanisms in Caco-2 cells, Adv. Drug Del. Rev. 22 (1996) 53–66.
[27] C.-M. Lehr, V.H. L Lee, Binding and transport of some bioadhesive plant lectins across Caco-2 cell monolayers, Pharm. Res. 10 (1993) 1796–1799.
[28] K.L. Audus, R.L. Bartel, I.J. Hildago, R.T. Borchardt, The use of cultured epithelial and endothelial cells for drug transport and metabolism studies, Pharm. Res. 7 (1996) 435–451.
[29] C. Coester, Nanoparticles and their Preparation Techniques. German Patent Application No. 10 041 340.1, 2004.
[30] C.A. Farrugia, M.J. Groves, Gelatin behavior in dilute aqueous solution: designing a nanoparticulate formulation, J. Pharm. Pharmacol. 51 (1999) 643–649.
[31] I. Hubatsch, G.E. Eva, R. Per Artursson, Determination of drug permeability and prediction of drug absorption in Caco-2 monolayers, Nat. Protoc. 2 (2007) 2111–2119.
[32] A. Braun, S. Hämmerle, K. Suda, B. Rothen-Rutishauser, M. Günthert, S.D. Krämer, H. Wunderli-Allenspach, Cell cultures as tools in biopharmacy, Eur. J. Pharm. Sci. 11 (2000) S51–S60.
[33] K.A. Foster, M. Yazdanian, K.L. Audus, Microparticulate uptake mechanisms of in vitro cell culture models of the respiratory epithelium, J. Pharm. Pharmacol. 53 (2001) 57–66.
[34] I. Behrens, A.I.V. Pena, M.J. Alonso, T. Kissel, Comparative uptake studies of bioadhesive and non-bioadhesive nanoparticles in human intestinal cell lines and rats, Pharm. Res. 19 (2002) 1185–1193.

[35] A. Knight, E. Hughson, C.R. Hopkins, D.F. Cutler, Membrane protein trafficking through the common apical endosome compartment of polarized Caco-2 cells, Mol. Biol. Cell 6 (1995) 597–610.
[36] D.J. Brayden, M.A. Jepson, A.W. Baird, Keynote review: intestinal Peyer's patch M cells and oral vaccine targeting, Drug Discov. Today 10 (2005) 1145–1157.
[37] S.D. Conner, S.L. Schmid, Regulated portals of entry into the cell, Nature 422 (2003) 37–44.
[38] S.-H. Liu, W.G. Mallet, F.M. Brodskt, Clathrin-mediated endocytosis, in: M. Marsh (Ed.), Endocytosis, Oxford University Press, New York, 2001, pp. 1–25.
[39] M. Maniak, Macropinocytosis, in: M. Marsh (Ed.), Endocytosis, Oxford University Press, New York, 2001, pp. 78–93.
[40] J.H. Eldridge, C.J. Hammond, J.A. Meulbroek, J.K. Staas, R.M. Gilley, T.R. Tice, Controlled vaccine release in the gut-associated lymphoid tissues. I. Orally administered biodegradable microspheres target the Peyer's patches, J. Control. Release 11 (1990) 205–214.
[41] A. des Rieux, V. Fievez, M. Garinot, Y.-J. Schneider, V. Préat, Nanoparticles as potential oral delivery systems of proteins and vaccines: a mechanistic approach, J. Control. Release 116 (2006) 1–27.